15

Recovery of Ammonia and Ketones from Biomass Wastes

Eri Fumoto[1], Teruoki Tago[2] and Takao Masuda[2]
[1]*Energy Technology Research Institute, National Institute of Advanced Industrial Science and Technology, 16-1, Onogawa, Tsukuba*
[2]*Division of Chemical Process Engineering, Faculty of Engineering, Hokkaido University, Sapporo, Japan*

1. Introduction

Huge amounts of biomass wastes, such as animal waste and sewage sludge, are produced continuously in farms and disposal plants. The most common method for treating these wastes is to use landfill and/or incineration methods that consume large amounts of energy and cause environmental problems such as air and soil pollution. Because biomass wastes contain nitrogen compounds and various hydrocarbons, a new alternative process to convert the wastes into useful chemicals is desirable.

Ammonia, one such chemical, has been used as a fertilizer, and increasing interest has focused on it as a hydrogen carrier. Ammonia is a liquid around 0.8 MPa at room temperature and offers significant hydrogen storage capacity (17.7 wt% hydrogen in ammonia). Hydrogen has been produced by the decomposition of ammonia with catalysts, such as ruthenium and nickel (Ganley et al., 2004; Liu et al., 2008; Wang et al., 2004; Yin et al., 2004, 2006; Zhen et al., 2008). Hence, the recovery of ammonia from biomass wastes is demanded. After the treatment for ammonia recovery, the remaining liquid wastes containing lower ammonia concentrations could be used as liquid fertilizer, whereas the high concentration of ammonia in raw biomass wastes causes eutrophication of the soil.

Biomass wastes also contain various hydrocarbons, and several methods exist, such as thermal cracking and fermentation, to convert these wastes into useful chemicals. Methane and hydrogen have been produced by the gasification of biomass wastes above 1000 K with the addition of steam or air (Gross et al., 2008; Nipattummakul et al., 2010). Supercritical water gasification is a method conducted under high pressure to produce hydrogen (Guo et al., 2010a). Fuel oil has been produced by the treatment of biomass wastes at relatively low temperatures of between 673 and 823 K (Shen et al., 2005). Anaerobic fermentation has produced methane (Guo et al., 2010b). The treatment of biomass wastes under moderate conditions is desirable because of the high moisture content of the wastes. Biomass wastes contain various oxygen-containing hydrocarbons, and thus the conversion of these hydrocarbons into useful chemicals, such as ketones, appears to be a promising approach. Acetone is used as a raw material for plastics, such as poly(methyl methacrylate) (PMMA) and polycarbonate (PC).

This chapter describes a new method, shown in Fig. 1, to recover useful chemicals, such as ammonia and ketones, from biomass wastes. Ammonia is recovered by the adsorption of nitrogen compounds in the waste, and oxygen-containing hydrocarbons in the waste are catalytically cracked to produce ketones.

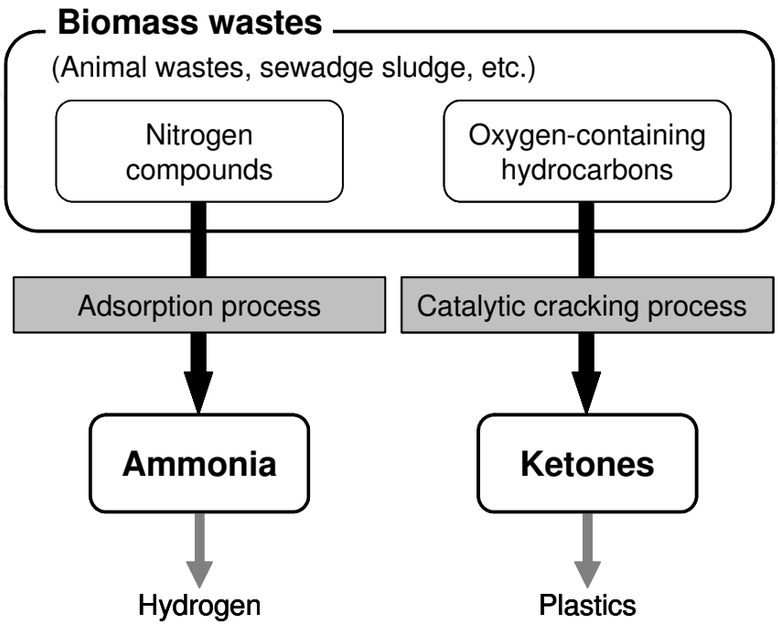

Fig. 1. Recovery method of ammonia and ketones from biomass wastes.

2. Recovery of ammonia

A promising method of ammonia recovery from biomass wastes includes two processes: the recovery of gaseous ammonia, which is generated by aeration of the biomass wastes, and the recovery of aqueous ammonium ions. Adequate adsorbents are required in both processes.

Some adsorbents, such as zeolite, sepiolite, and activated carbon, have been used to recover ammonia gas (Bernal and Lopez-Real, 1993; Park et al., 2005). The maximum amounts of ammonia adsorption on zeolite and sepiolite were approximately 0.8 mol-N/kg-zeolite and 0.3 mol-N/kg-sepiolite (Bernal and Lopez-Real, 1993). Zeolite and sepiolite have also been used to recover ammonium ions in liquid phase (Balci, 2004; Bernal and Lopez-Real, 1993; Yusofa et al., 2010). The maximum adsorption of ammonium ions on zeolite Y was approximately 2.4 mol-N/kg-zeolite (Yusofa et al., 2010).

The precipitation of magnesium ammonium phosphate ($MgNH_4PO_4 \cdot 6H_2O$, MAP) is a useful process for removing ammonium ions in liquid phase (Chimenos et al., 2003; Diwania et al., 2007; Nelson et al., 2003; Stratful et al., 2001). MAP can be precipitated by adding magnesium and phosphate to ammonium solution at a pH above 7. Sugiyama et al. (2005, 2007) reported that an adsorbent derived from MAP was useful for the recovery of ammonium ions from aqueous solution. Ammonia was removed from MAP by thermal treatment above 353 K, yielding a solid, which is the adsorbent for the recovery of aqueous ammonium ions.

The application of MAP-derived adsorbents to both the adsorption process of gaseous ammonia and aqueous ammonium ions could be a promising approach to recover ammonia

from biomass wastes. The recovery process of ammonia from biomass wastes in liquid or gas phase is depicted in Fig. 2. Thermal treating of MAP produces ammonia, water, and the adsorbent, which is $Mg(NH_3)_{1-X}HPO_4$. The behaviors of adsorption of gaseous ammonia and aqueous ammonium ions and desorption of ammonia are discussed in this section.

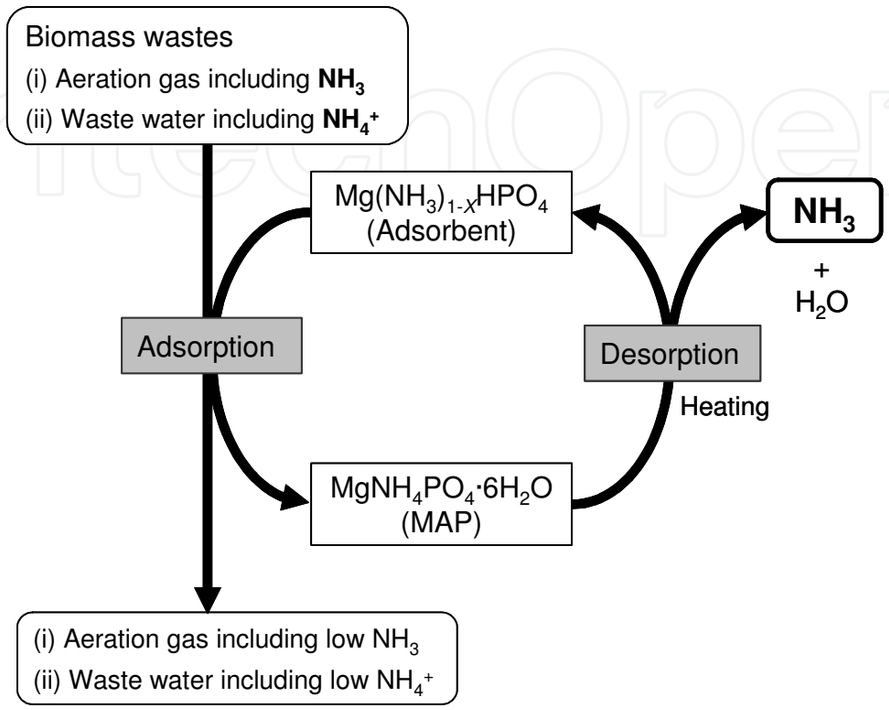

Fig. 2. Ammonia recovery process from biomass wastes using MAP-derived adsorbents.

2.1 Adsorbents derived from MAP

Ammonia can be removed from MAP by heating. Sugiyama et al. (2005) reported that the weight of MAP decreased drastically in the temperature range of 350–400 K due to the elimination of ammonia and water when MAP was heated. The nitrogen content in MAP was reduced by heating, and ammonia was largely eliminated from MAP in the temperature range of 340–360 K (Fumoto et al., 2009). Table 1 shows the remaining nitrogen content in the solids treated at 378 K and 573 K for 24 h in a thermostatic oven. Approximately 70% and 90% of ammonia was eliminated from MAP by thermal treatment at 378 K and 573 K, respectively (Fumoto et al., 2009). The remaining nitrogen content and the amount of weight loss indicate that the adsorption capacity of ammonia onto the solids treated at 378 K and 573 K was 3.6 and 6.0 mol-N/kg-solid, respectively.

Treatment temperature [K]	Remaining nitrogen content [mol-N/mol-Mg]	Surface area [m^2/g]
378	0.30	204
573	0.090	111

Table 1. Remaining nitrogen content and BET surface area of solids obtained by thermal treatment of MAP (Fumoto et al., 2009).

Figures 3 and 4 illustrate the nitrogen sorption isotherms and pore volume distributions of the solids obtained by treating MAP at 378 K and 573 K. The Brunauer-Emmett-Teller (BET) surface area of the solids was calculated and is given in Table 1. The sorption isotherms exhibited hysteresis, indicating that the solids have pores. The solid treated at 378 K had several nanopores, and the surface area of this solid was larger than that of the solid treated at 573 K (Fumoto et al., 2009). These results suggest that the solid treated at 378 K may be a suitable adsorbent for recovering gaseous ammonia and aqueous ammonium ions.

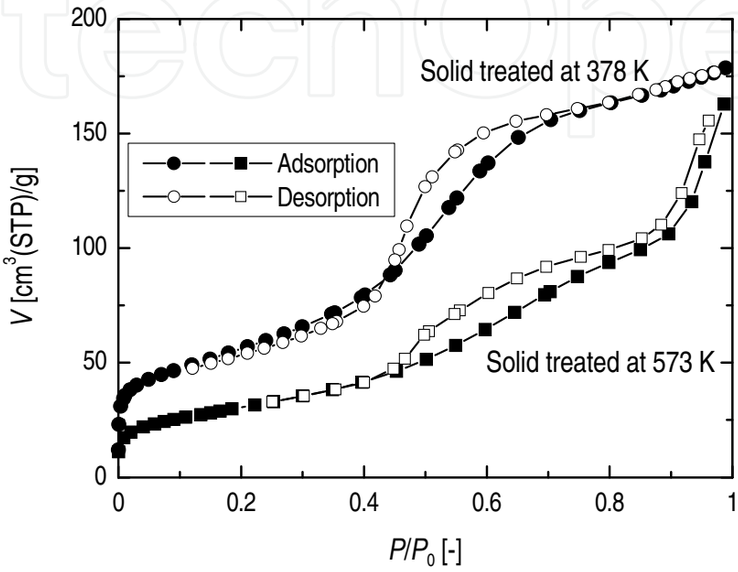

Fig. 3. Nitrogen sorption isotherms of solids obtained by treating MAP at 378 K and 573 K (Fumoto et al., 2009).

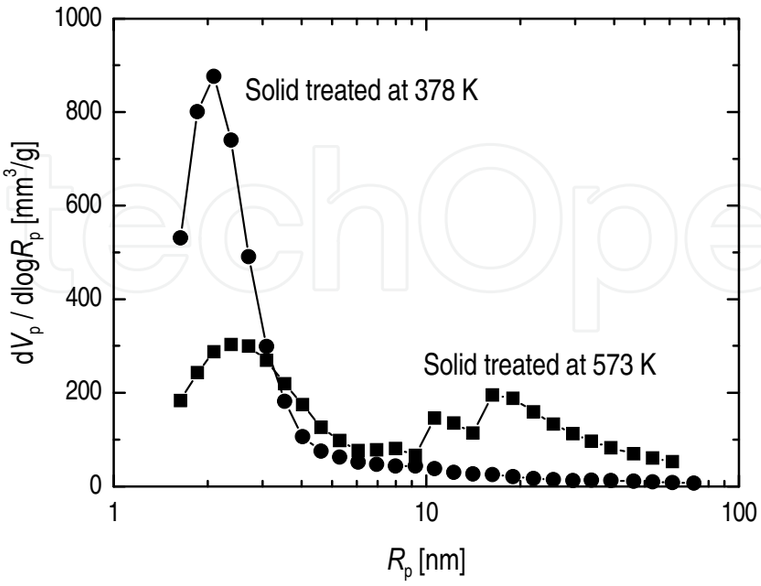

Fig. 4. Pore volume distribution of solids obtained by treating MAP at 378 K and 573 K (Fumoto et al., 2009).

2.2 Gas phase adsorption of ammonia on MAP-derived adsorbents

The adsorption of gaseous ammonia on the adsorbent obtained by treating MAP at 378 K was investigated. The adsorbent, loaded in a stainless steel column, was controlled at 313–353 K, and the experiment of ammonia adsorption was conducted by introducing a mixture of ammonia, hydrogen, and argon. The concentration of ammonia in the inlet gas, C_0, was 2.4 mol/m^3. The outlet gas, including ammonia, hydrogen, and argon, was monitored with a quadrupole mass spectrometer (Q-MS). The mass numbers were chosen as 15, 2, and 40, to detect ammonia, hydrogen, and argon, respectively. Hydrogen was introduced to determine the travel time of the gas from the inlet to the Q-MS. In a preliminary experiment, hydrogen and argon were confirmed to not be adsorbed on the adsorbent.

Figure 5 depicts the effect of temperature on the amount of adsorption of gaseous ammonia on the adsorbent obtained by treating MAP at 378 K. Breakthrough curves of ammonia adsorption were obtained from the measured ammonia concentration in the outlet gas, C_t. The amount of ammonia adsorption, q, was calculated according to Eq. (1).

$$q = \frac{v \cdot C_0}{W} \int_0^{\infty} (1 - C_t / C_0)\,\mathrm{d}t\,, \tag{1}$$

where v is the flow rate and W is the weight of the adsorbent. The lower the temperature is, the larger the amount of ammonia is adsorbed. The maximum adsorption amount was 2.56 mol-N/kg-adsorbent (Fumoto et al., 2009), which is much larger than that on zeolite (0.8 mol-N/kg-zeolite; Bernal and Lopez-Real, 1993).

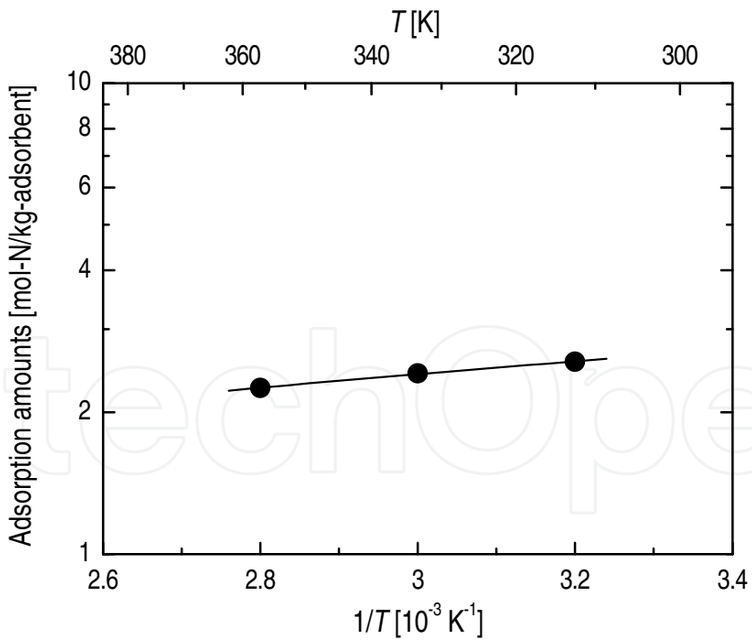

Fig. 5. Effect of temperature on the amount of gaseous ammonia adsorbed on the adsorbent obtained by treating MAP at 378 K (Fumoto et al., 2009).

Figure 6 presents an adsorption isotherm of gaseous ammonia at 313 K. The adsorbent was obtained by thermal treatment of MAP at 378 K. The amount of adsorption of ammonia was proportional to the ammonia concentration, indicating Henry-type adsorption (Fumoto et

al., 2009). The adsorption energy, calculated from the data of Arrhenius plots in Fig. 5, was low (–3.0 kJ/mol). These results suggest that gaseous ammonia was physically adsorbed on the adsorbent.

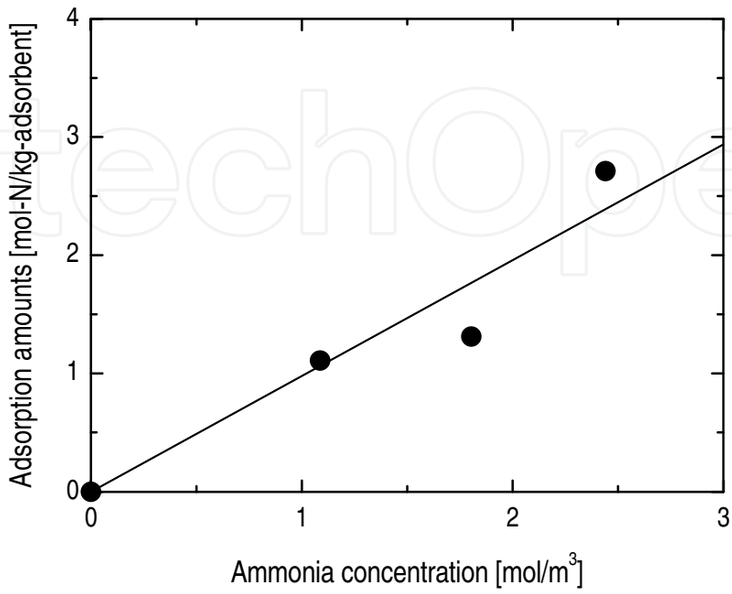

Fig. 6. Adsorption isotherm of gaseous ammonia at 313 K on the adsorbent obtained by treating MAP at 378 K (Fumoto et al., 2009).

2.3 Liquid phase adsorption of ammonium ions on MAP-derived adsorbents

The adsorption of ammonium ions on MAP-derived adsorbents from ammonia water was investigated. The ammonium concentration was 500–12000 ppm and the pH of the ammonia water was adjusted to 11 by adding sodium hydroxide. The adsorbent obtained by treating MAP at 378 K and 573 K was added to the ammonia water at a weight ratio of adsorbents to ammonia water of 1:100, and the ammonium concentration was analyzed after 1 h of stirring at room temperature.

Figure 7 depicts the adsorption isotherms of ammonium ions on the adsorbent from ammonia water at room temperature; the calculated adsorption capacity of ammonium ions is also shown. A large amount of ammonium ions became adsorbed on the adsorbent treated at 378 K (Fumoto et al., 2009), whereas the maximum adsorption amount on zeolite Y was approximately 2.4 mol-N/kg-zeolite (Yusofa et al., 2010). The experimental value of the adsorbed ammonium ions on the adsorbent treated at 378 K was larger than the calculated value. An adsorption isotherm of ammonium ions on the adsorbent treated at 378 K shows Langmuir-type adsorption, indicating chemical adsorption. Figure 8 shows X-ray diffraction (XRD) patterns of MAP and the adsorbent treated at 378 K before and after the adsorption of ammonium ions. The pattern of the adsorbent treated at 378 K shows peaks corresponding to $MgNH_4PO_4 \cdot H_2O$. Sugiyama et al. (2005) reported that MAP was converted to amorphous $MgHPO_4$ by thermal treatment below 773 K. These results suggest that the adsorbent consisted of amorphous $MgHPO_4$ and $MgNH_4PO_4 \cdot H_2O$. The adsorbent after the adsorption of ammonium ions exhibited peaks similar to those of the MAP (Fumoto et al., 2009). Hence, ammonium ions were adsorbed on the site of $MgHPO_4$ of the adsorbent, and the MAP was re-formed in the presence of water.

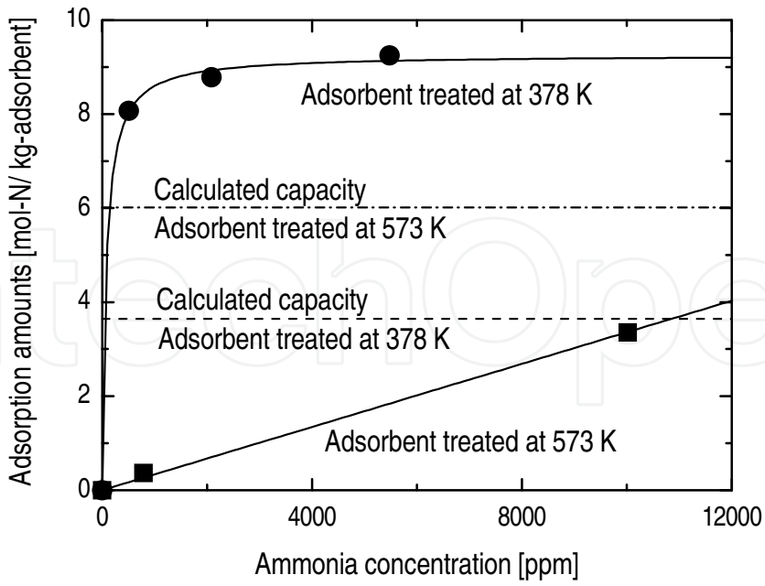

Fig. 7. Adsorption isotherms of ammonium ions at room temperature on the adsorbent obtained by treating MAP at 378 K and 573 K (Fumoto et al., 2009).

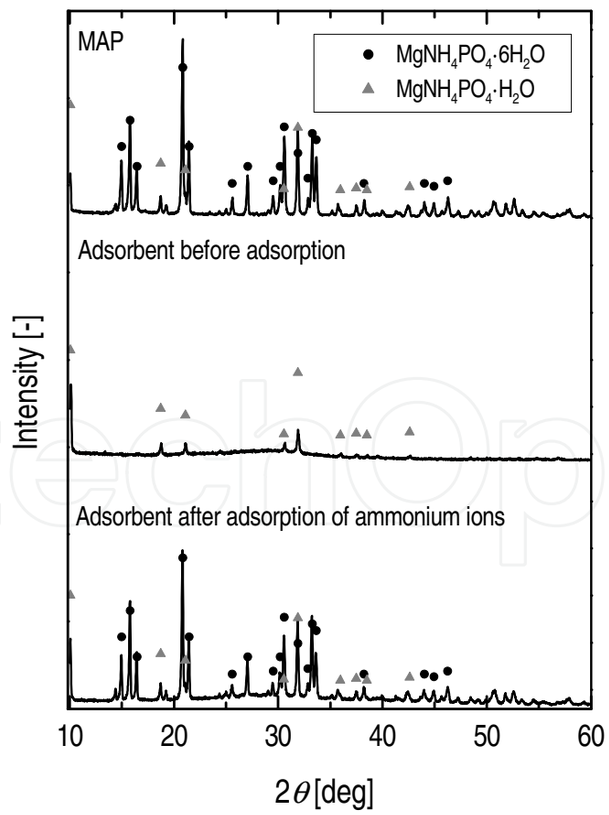

Fig. 8. XRD patterns of MAP and adsorbent treated at 378 K before and after the adsorption of ammonium ions (Fumoto et al., 2009).

The amount of ammonium ions adsorbed on the adsorbent treated at 573 K was significantly less than that of the adsorbent treated at 378 K, as shown in Fig. 7. Furthermore, the experimental value was less than the calculated capacity in the case of the adsorbent treated at 573 K. The fewer nanopores and smaller surface area of the adsorbent treated at 573 K caused the lower adsorption of ammonium ions. The surface chemical properties of the adsorbent may be different between the adsorbents treated at 378 K and 573 K. Consequently, the adsorbent obtained by treating MAP at 378 K was more suitable for the adsorption of ammonium ions.

2.4 Recovery of ammonium ions from animal wastes

The feasibility of recovering ammonia from biomass wastes was demonstrated using cow urine. The urine was pretreated under a hydrothermal condition at 573 K for 1 h to convert nitrogen compounds in the urine into ammonium ions. The pH was adjusted to 10.5 by adding sodium hydroxide and the adsorbent treated at 378 K was added to the pretreated urine at an adsorbent to urine weight ratio of 1:10. The nitrogen concentration was analyzed after 1 h of stirring.

	Recovery yield [mol%-N]	Impurities deposition [mol/mol]	
		C/N	S/N
Pretreated urine	56.9	0.103	0
Untreated urine	65.2	0.486	0.0196

Table 2. Nitrogen recovery yield and impurities deposited on the adsorbent from urine solution (Fumoto et al., 2009).

Table 2 lists the nitrogen recovery yield and the impurities deposited on the adsorbent from the urine; the results obtained using untreated urine are also shown. More than 50% of the nitrogen was recovered from the urine using the adsorbent obtained by treating MAP at 378 K (Fumoto et al., 2009). The nitrogen concentration of the urine decreased to 2000 ppm after the recovery experiment, and the remaining liquid wastes could be used as liquid fertilizer because the liquid contained a low concentration of ammonia.

The nitrogen recovered from pretreated urine corresponded well with ammonium ions because the carbon deposition on the adsorbent was small, as shown in Table 2. In contrast, some carbon was deposited on the adsorbent from the untreated urine, indicating that most of the nitrogen adsorbed on the adsorbent was urea. Furthermore, no sulfur was deposited on the adsorbent from the pretreated urine, which contained sulfur. Therefore, large amounts of ammonia were recovered from the biomass wastes using this method without impurities.

2.5 Desorption of ammonia from solids adsorbing ammonia

The recovery of ammonia by thermal treatment of the solids adsorbing gaseous ammonia and aqueous ammonium ions was examined. The MAP structure was re-formed after the adsorption of ammonium ions in liquid phase. Hence, the solid adsorbing gaseous ammonia and MAP were loaded in the stainless column, followed by heating the column at a rate of 1 K/min in an argon stream. The solid, which was obtained by treating MAP at 378 K, was used after the adsorption of gaseous ammonia. The ammonia and steam eliminated from the solid and MAP was measured by Q-MS. The mass numbers were chosen as 15, 18, and 40 to detect ammonia, steam, and argon, respectively.

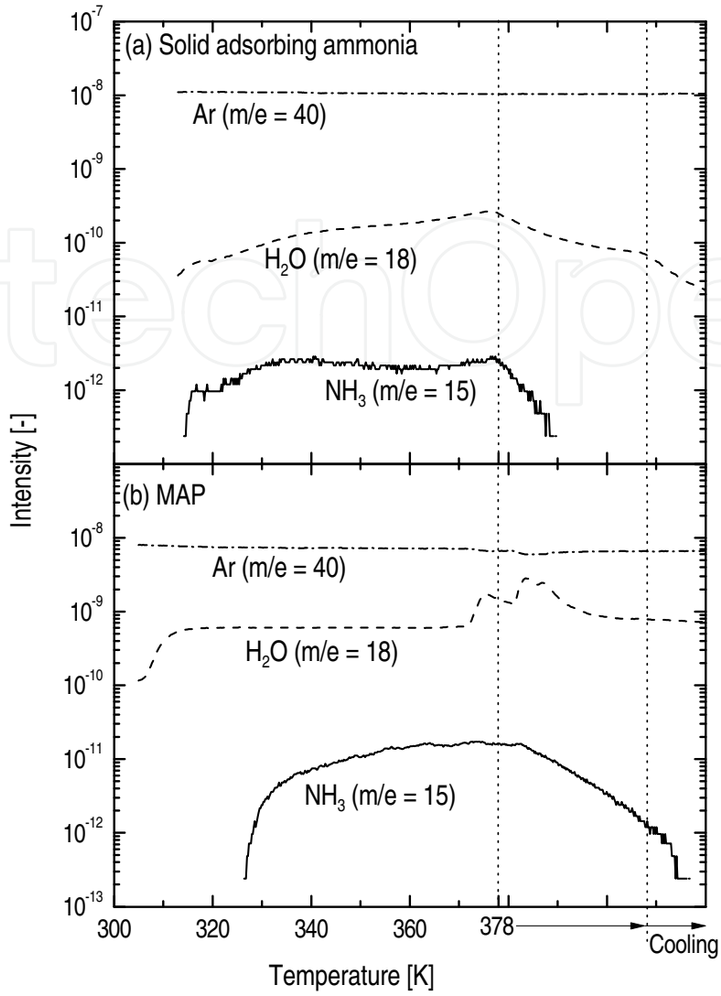

Fig. 9. Gas fractions generated from the solid adsorbing gaseous ammonia and MAP.

Figure 9 describes the gas fractions eliminated from the solids adsorbing gaseous ammonia and MAP. Ammonia was eliminated when these samples were heated. The solid adsorbing gaseous ammonia released ammonia at a relatively lower temperature compared with the MAP, suggesting the physical adsorption of gaseous ammonia. Steam may be desorbed from moisture adsorbed on the surface of the solids and crystallization water of MAP. These results indicate that ammonia could be recovered by thermal treatment of the solids after the adsorption of gaseous ammonia and ammonium ions. Hence, the adsorbent derived from MAP could be used repeatedly.

2.6 Stability of adsorbents for repeated use

The adsorbents derived from MAP are expected to be reused for the recycling process of adsorption and desorption of ammonia. Sugiyama et al. (2005) reported that the removal of ammonium ions in the second run was about 80% of that in the first run when an ammonium removal experiment from aqueous ammonium ions was conducted using adsorbent derived from MAP. The stability of the adsorbents was investigated for repeated use in gaseous ammonium adsorption.

Figure 10 illustrates the change in amounts of adsorbed ammonia on the adsorbents when the sequence of ammonia adsorption and desorption was repeated. After the adsorption of gaseous ammonia at 313 K on the adsorbent obtained by treating MAP at 378 K, the adsorbent was heated to 378 K to eliminate the ammonia, and it was used repeatedly for the adsorption experiment. The amount of ammonia hardly changed in the adsorption/desorption sequence. The pore structure of the adsorbent was almost maintained. Accordingly, this adsorbent is useful for the recovery of ammonia with repeated sequences of adsorption and desorption.

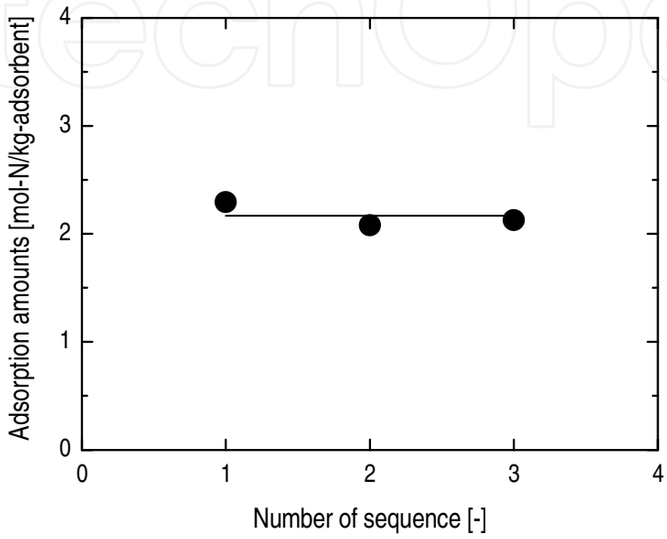

Fig. 10. Change in the amount of adsorbed gaseous ammonia with repeated sequences of ammonia adsorption and desorption.

3. Recovery of ketones

The conversion of hydrocarbons in biomass wastes into useful chemicals is also a promising method. Figure 11 depicts the recovery process of ketones from biomass wastes. To solubilize the solid biomass wastes, such as sewage sludge, the wastes are hydrothermally treated, producing black water. The obtained black water consists of oxygen-containing hydrocarbons and a large amount of water. Some impurities, such as nitrogen and sulfur, are contained in the black water. The conversion of black water into useful chemicals requires catalysts having the following properties: a strong ability to decompose the hydrocarbons in the black water, stable activity in the presence of water, and resistance to the deposition of impurities contained in the black water.

Zirconia-supporting iron oxide catalysts are effective for the decomposition of oil palm waste (Masuda et al., 2001) and petroleum residual oil (Fumoto et al., 2004) in a steam atmosphere. Oil palm waste can be converted to a mixture containing phenol, acetone, and butanone using the catalyst. Hydrocarbons in oil palm waste and petroleum residual oil react with active oxygen species generated from steam on the iron oxide catalyst. Zirconia promotes the generation of the active oxygen species from steam.

The production of ketones from sewage-derived black water was investigated. Figure 12 presents the conversion of oxygen-containing hydrocarbons to ketones with the zirconia-supporting iron oxide catalysts. The active oxygen species generated from steam could react with the hydrocarbons.

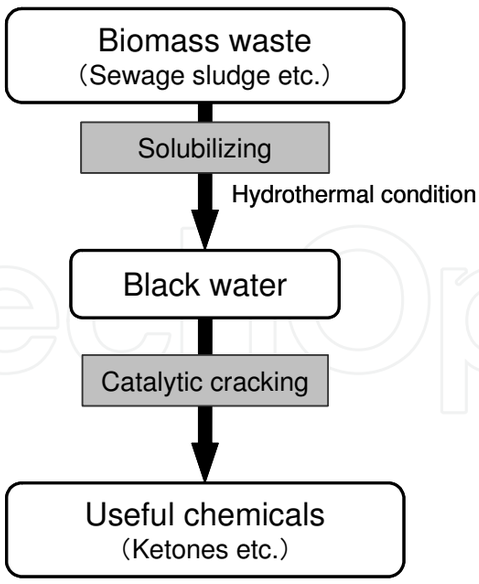

Fig. 11. Recovery of ketones from biomass wastes.

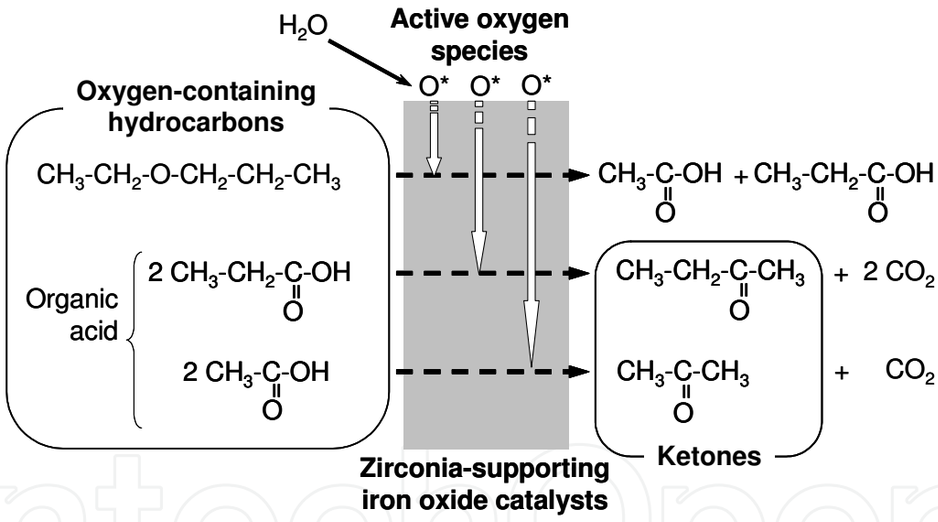

Fig. 12. Reaction mechanism of oxygen-containing hydrocarbons with zirconia-supporting iron oxide catalysts.

3.1 Production of ketones from sewage sludge

Catalytic cracking of sewage-derived black water was investigated under superheating steam conditions. The black water was obtained by the hydrothermal treatment of digested sewage sludge at 573 K. The moisture content of the black water was 98 wt%. The zirconia-supporting iron oxide catalyst was prepared by a coprecipitation method using $FeCl_3 \cdot 6H_2O$ and $ZrOCl_3 \cdot 8H_2O$, yielding the catalyst denoted as Zr(*Y*)-FeO_X, where *Y* is the amount of the supported zirconia by weight percent. The catalytic cracking of sewage-derived black water was carried out at 523 K under 2 MPa for 2 h using a batch autoclave reactor loaded with 0.2 g of catalyst and 3.2 g of black water. The product was analyzed by gas chromatography (GC).

Figure 13 illustrates the product yield after the reaction of black water with Zr(*Y*)-FeO_X catalysts. The catalysts were active for producing acetone from black water (Fumoto et al., 2006a). The yield of acetone produced from black water increased with increasing zirconia content and reached the maximum value at 7.7 wt% zirconia content. Figure 14 shows the desorption rate of hydrogen generated by the decomposition of steam when the catalysts were heated after the pre-adsorption of steam on the catalysts. The catalyst supporting zirconia exhibited higher steam decomposition activity, even at lower temperatures, producing hydrogen (Masuda et al., 2001). Simultaneously, active oxygen species were generated from steam. These oxygen species spill over to the surface of iron oxide, and oxygen-containing hydrocarbons in black water react with the active oxygen species on the iron oxide. The yield of acetone produced in the reaction with the Zr(15.8)- FeO_X catalyst was less than that in case of the Zr(7.7)-FeO_X catalyst. The active sites on the iron oxide may be covered with the excessively supported zirconia. Consequently, the largest amount of acetone was produced by the reaction of sewage-derived black water with the Zr(7.7)-FeO_X catalyst.

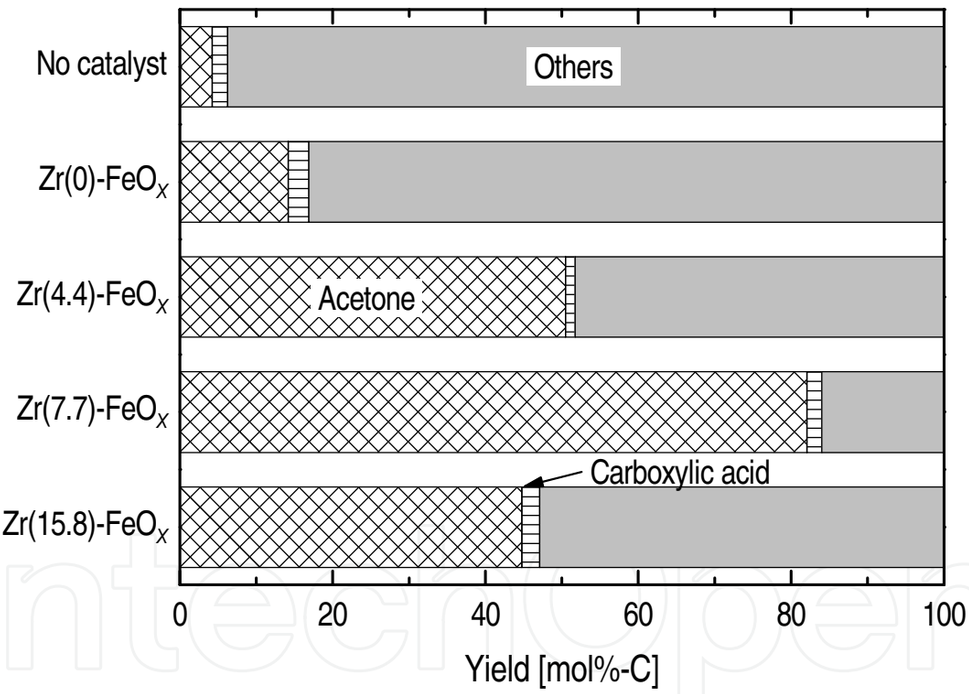

Fig. 13. Product yield of the reaction of black water derived from sewage sludge with Zr(*Y*)-FeO_X catalysts (Fumoto et al., 2006a).

3.2 Durability of zirconia-supporting iron oxide catalysts

High durability of the catalysts is demanded for their long-term use. The black water contains impurities, such as nitrogen and sulfur, which have the potential of poisoning the catalysts. Nitrogen compounds could be removed by adsorption using the MAP-derived adsorbent. To examine the durability of the catalysts, an accelerated deterioration test using petroleum residual oil, which contained sulfur, was conducted.

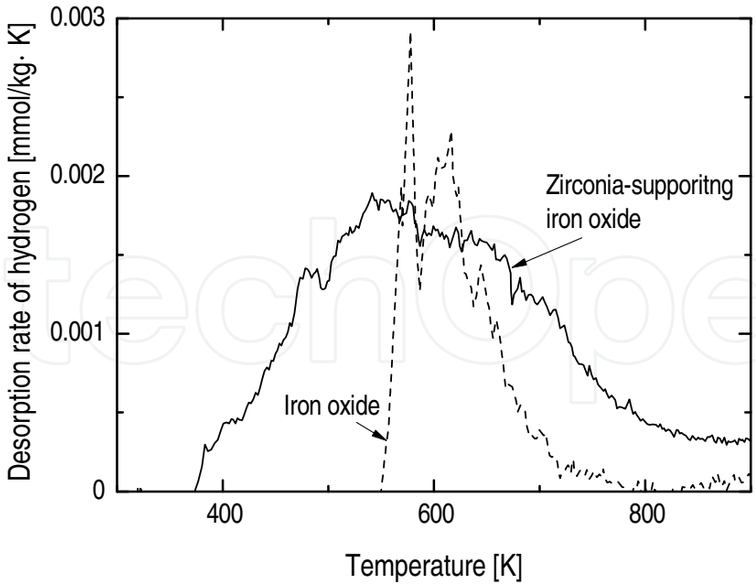

Fig. 14. Desorption rate of hydrogen from steam when the catalyst was heated after the pre-adsorption of steam on the catalysts (Masuda et al., 2001).

Three types of catalysts, Zr/FeO_X, $Zr/Al\text{-}FeO_X$, and $Zr\text{-}Al\text{-}FeO_X$, were prepared. Zirconia was supported on the iron oxide, which was generated from the treatment of *a*-FeOOH with steam, by impregnation using $ZrOCl_3 \cdot 8H_2O$, yielding the Zr/FeO_X catalyst. The complex metal oxide of aluminum and iron was obtained by a coprecipitation method using $FeCl_3 \cdot 6H_2O$ and $Al_2(SO_4)_3 \cdot 14\text{-}18H_2O$, and zirconia was supported on the complex metal oxide by impregnation, yielding the $Zr/Al\text{-}FeO_X$ catalyst. The $Zr\text{-}Al\text{-}FeO_X$ catalyst was prepared by coprecipitation using $FeCl_3 \cdot 6H_2O$, $Al_2(SO_4)_3 \cdot 14\text{-}18H_2O$, and $ZrOCl_3 \cdot 8H_2O$. The loaded amount of zirconia was 7.7 wt% and the atomic fraction of Al in $Al\text{-}FeO_X$ was 0.079. The catalytic cracking of atmospheric residual oil was conducted in a steam atmosphere at 773 K under atmospheric pressure using a fixed bed reactor loaded with the catalyst. The product oil was analyzed by GC and gel permeation chromatography (GPC).

Figure 15 depicts the change in catalytic activity for the decomposition of heavy oil after the sequence of reaction of residual oil and regeneration of the catalyst. The reaction rate constant, *k*, was calculated according to Eq. (2):

$$\frac{\mathrm{d}f_{\mathrm{C30+}}}{\mathrm{d}(W/F_{\mathrm{R}})} = -k \cdot f_{\mathrm{C30+}}{}^{2}, \tag{2}$$

where f_{C30+} represents the weight fraction of heavy oil (carbon number above 30), and W/F_R is the time factor corresponding to the ratio of the weight of catalyst to the flow rate of residual oil. The activity of the Zr/FeO_X catalyst decreased when the sequence of reaction and regeneration was repeated (Fumoto et al., 2006b). The peeling of zirconia from iron oxide due to structural changes of the iron oxide catalyst caused the deactivation. The $Zr/Al\text{-}FeO_X$ catalyst was not deactivated after the reaction and regeneration sequence. The addition of alumina prevented the structural change of iron oxide. When the reaction was repeated without regeneration, the $Zr\text{-}Al\text{-}FeO_X$ catalyst maintained high activity (Fumoto et al., 2006c), whereas the activity of the $Zr/Al\text{-}FeO_X$ catalyst decreased without the

regeneration. The lattice oxygen of iron oxide was consumed during the reaction, causing a phase change of the iron oxide of Zr/FeO_X and Zr/Al-FeO_X catalysts from hematite to magnetite. Hence, the catalyst was regenerated by calcinations. In contrast, the hematite of the Zr-Al-FeO_X catalyst was maintained after the reaction, leading to stable activity without regeneration. No correlation was observed between the activity of the catalyst and the deposition of impurities from residual oil. Accordingly, the Zr-Al-FeO_X catalyst could be useful for long-term application in the conversion process of biomass wastes.

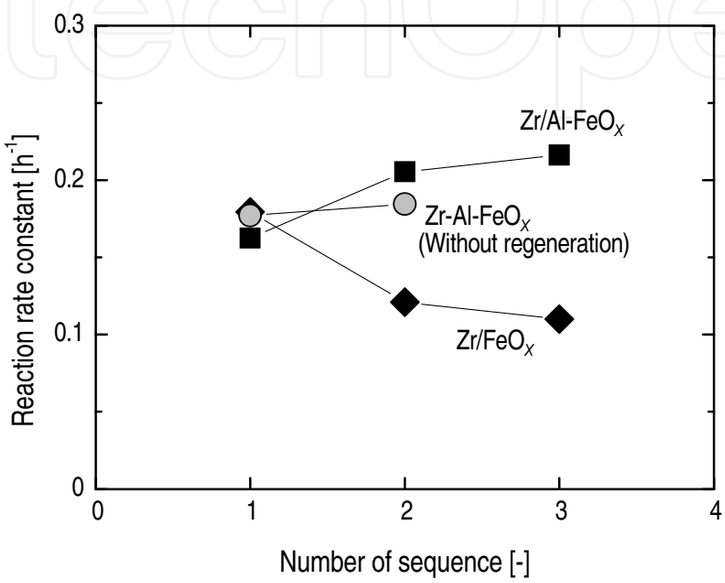

Fig. 15. Change in catalytic activity for the decomposition of heavy oil with a repeated sequence of reaction and regeneration (Fumoto et al., 2006b, 2006c).

4. Conclusion

New methods for recovering ammonia and ketones from biomass wastes were investigated. The gaseous ammonia and aqueous ammonium ions were adsorbed effectively on the adsorbent obtained by treating MAP at 378 K. The adsorption of gaseous ammonia and aqueous ammonium ions was physical and chemical adsorption, respectively. The ammonia could be recovered by thermal treating of the adsorbent after the adsorption of ammonia and ammonium ions, suggesting that the adsorbent is useful for repeated use of the ammonia adsorption/desorption sequence. Large amounts of ammonia were recovered from hydrothermally treated cow urine using the adsorbent, without impurities contained in the urine. Biomass wastes also contain various hydrocarbons. The solid wastes, such as sewage sludge, were solubilized by hydrothermal treatment, producing black water, and catalytic cracking of the black water was conducted. As a result, large amounts of acetone were produced with the zirconia-supporting iron oxide catalyst. Oxygen-containing hydrocarbons reacted with the active oxygen species generated from steam on the iron oxide catalyst. Supported zirconia promoted the generation of the active species. Hence, the yield of acetone increased with the increasing zirconia content in the catalyst. Furthermore, the complex metal oxide catalyst of iron, zirconium, and aluminum showed stable activity

for the decomposition of heavy oil. Accordingly, the catalyst may be suitable for the catalytic cracking of biomass wastes.

5. References

Balci, S. (2004). Nature of Ammonium Ion Adsorption by Sepiolite: Analysis of Equilibrium Data with Several Isotherms. *Water Res.*, Vol.38, No.5, (March 2004), pp. 1129-1138, ISSN 0043-1354

Bernal, M. P. & Lopez-Real, J. M. (1993). Natural Zeolites and Sepiolite as Ammonium and Ammonia Adsorbent Materials. *Bioresour. Technol.*, Vol.43, No.1, (1993), pp. 27-33, ISSN 0960-8524

Chimenos, J. M., Fernandez, A. I., Villalba, G., Segarra, M., Urruticoechea, A., Artaza, B. & Espiell, F. (2003). Removal of Ammonium and Phosphates from Wastewater Resulting from the Process of Cochineal Extraction using MgO-Containing By-Product. *Water Res.*, Vol.37, No.7, (April 2003), pp. 1601-1607, ISSN 0043-1354

Diwania, G. E., Rafiea, S. E., Ibiaria, N. N. E. & Ailab, H. I. E. (2007). Recovery of Ammonia Nitrogen from Industrial Wastewater Treatment as Struvite Slow Releasing Fertilizer. *Desalin.*, Vol.214, No.1-3, (August 2007), pp. 200–214, ISSN 0011-9164

Fumoto, E., Tago, T., Tsuji, T. & Masuda, T. (2004). Recovery of Useful Hydrocarbons from Petroleum Residual Oil by Catalytic Cracking with Steam over Zirconia-Supporting Iron Oxide Catalyst. *Energy Fuels*, Vol.18, No.6, (November-December 2004), pp. 1770-1774, ISSN 0887-0624

Fumoto, E., Mizutani, Y., Tago, T. & Masuda, T. (2006a). Production of Ketones from Sewage Sludge over Zirconia-Supporting Iron Oxide Catalysts in a Steam Atmosphere. *Appl. Catal. B*, Vol.68, No.3-4, (November 2006), pp. 154-159, ISSN 0926-3373

Fumoto, E., Tago, T. & Masuda, T. (2006b). Production of Lighter Fuels by Cracking Petroleum Residual Oils with Steam over Zirconia-Supporting Iron Oxide Catalysts. *Energy Fuels*, Vol.20, No.1, (January-February 2006), pp. 1-6, ISSN 0887-0624

Fumoto, E., Tago, T. & Masuda, T. (2006c). Recovery of Lighter Fuels from Petroleum Residual Oil by Oxidative Cracking with Steam over Zr-Al-FeOx Catalyst. *Chem. Lett.*, Vol.35, No.9, (September 2006), pp. 998-999, ISSN 0366-7022

Fumoto, E., Tago, T. & Masuda, T. (2009). Recovery of Ammonia from Biomass Waste by Adsorption on Magnesium Phosphate Derived from Magnesium Ammonium Phosphate. *J. Chem. Eng. Jpn.*, Vol.42, No.3, (2009), pp.184-190, ISSN 0021-9592

Ganley, J. C., Thomas, F. S., Seebauer, E. G. & Masel, R. I. (2004). A Priori Catalytic Activity Correlations the Difficult Case of Hydrogen Production from Ammonia. *Catal. Lett.*, Vol.96, No.3-4, (July 2004), pp. 117-122, ISSN 1011-372X

Gross, B., Eder, C., Grziwa, P., Horst, J. & Kimmerle, K. (2008). Energy Recovery from Sewage Sludge by Means of Fluidised Bed Gasification. *Waste Manage.*, Vol.28, No.10, (2008), pp. 1819-1826, ISSN 0956-053X

Guo, Y., Wang, S. Z., Xu, D. H., Gong, Y. M., Ma, H. H. & Tang, X. Y. (2010a). Review of Catalytic Supercritical Water Gasification for Hydrogen Production from Biomass. *Renewable Sustainable Energy Rev.*, Vol.14, No.1, (January 2010), pp. 334–343, ISSN 1364-0321

Guo, X. M., Trably, E., Latrille, E., Carrère, H. & Steyer, J. P. (2010b). Hydrogen Production from Agricultural Waste by Dark Fermentation: A Review. *Int. J. Hydrogen Energy*, Vol.35, No.19, (October 2010), pp. 10660-10673, ISSN 0360-3199

Liu, H. C., Wang, H., Shen, J. G., Sun, Y, & Liu, Z. M. (2008). Preparation, Characterization and Activities of the Nano-Sized Ni/SBA-15 Catalyst for Producing COx-Free

Hydrogen from Ammonia. *Appl. Catal. A*, Vol.337, No. 2, (March 2008), pp. 138-147, ISSN 0926-860X

Masuda, T., Kondo, Y., Miwa, M., Shimotori, T., Mukai, S. R., Hashimoto, K., Takano, M., Kawasaki, S. & Yoshida, S. (2001). Recovery of Useful Hydrocarbons from Oil Palm Waste Using ZrO_2 Supporting FeOOH Catalyst. *Chem. Eng. Sci.*, Vol.56, No.3, (February 2001), pp. 897-904, ISSN 0009-2509

Nelson, N. O., Mikkelsen, R. L. & Hesterberg, D. L. (2003). Struvite Precipitation in Anaerobic Swine Lagoon Liquid: Effect of pH and Mg : P Ratio and Determination of Rate Constant. *Bioresour. Technol.*, Vol.89, No.3, (September 2003), pp. 229-236, ISSN 0960-8524

Nipattummakul, N., Ahmed, I. I., Kerdsuwan, S. & Gupta, A. K. (2010). Hydrogen and Syngas Production from Sewage Sludge via Steam Gasification. *Int. J. Hydrogen Energy*, Vol.35, No.21, (November 2010), pp. 11738-11745, ISSN 0360-3199

Park, S. J. & Kim, B. J. (2005). Ammonia Removal of Activated Carbon Fibers Produced by Oxyfluorination. *J. Colloid Interface Sci.*, Vol.291, No.2, (November 2005), pp. 597-599, ISSN 0021-9797

Shen, L. & Zhang, D. K. (2005). Low-Temperature Pyrolysis of Sewage Sludge and Putrescible Garbage for Fuel Oil Production. *Fuel*, Vol.84, No.7-8, (May 2005), pp. 809-815, ISSN 0016-2361

Stratful, I., Scrimshaw, M. D. & Lester, J. N. (2001). Conditions Influencing the Precipitation of Magnesium Ammonium Phosphate. *Water Res.*, Vol.35, No.17, (December 2001), pp. 4191-4199, ISSN 0043-1354

Sugiyama, S., Yokoyama, M., Ishizuka, H., Sotowa, K., Tomida, T. & Shigemoto, N. (2005). Removal of Aqueous Ammonium with Magnesium Phosphates Obtained from the Ammonium-Elimination of Magnesium Ammonium Phosphate. *J. Colloid Interface Sci.*, Vol.292, No.1, (December 2005), pp. 133-138, ISSN 0021-9797

Sugiyama, S., Yokoyama, M., Fujii, M., Seyama, K. & Sotowa, K. (2007). Recycling of Thin-Layer of Magnesium Hydrogenphosphate for Removal and Recovery of Aqueous Ammonium. *J. Chem. Eng. Jpn.*, Vol.40, No.2, (February 2007), pp. 198-201., ISSN 0021-9592

Wang, S. J., Yin, S. F., Li, L., Xu, B. Q., Ng, C. F. & Au, C. T. (2004). Investigation on Modification of Ru/CNTs Catalyst for the Generation of COx-Free Hydrogen from Ammonia. *Appl. Catal. B*, Vol.52, No.4, (October 2004), pp. 287-299, ISSN 0926-3373

Yin, S. F., Xu, B. Q., Zhou, X. P. & Au, C. T. (2004). A Mini-Review on Ammonia Decomposition Catalysts for On-Site Generation of Hydrogen for Fuel Cell Applications. *Appl. Catal. A*, Vol.277, No.1-2, (December 2004), pp. 1-9, ISSN 0926-860X

Yin, S. F., Xu, B. Q., Wang, S. J. & Au, C. T. (2006). Nanosized Ru on High-Surface-Area Superbasic ZrO_2-KOH for Efficient Generation of Hydrogen via Ammonia Decomposition. *Appl. Catal. A*, Vol.301, No.2, (February 2006), pp. 202-210, ISSN 0926-860X

Yusofa, A. M., Keata, L. K., Ibrahimb, Z., Majida, Z. A. & Nizamb, N. A. (2010). Kinetic and Equilibrium Studies of the Removal of Ammonium Ions from Aqueous Solution by Rice Husk Ash-Synthesized Zeolite Y and Powdered and Granulated Forms of Mordenite. *J. Hazard. Mater.*, Vol.174, No.1-3, (February 2010), pp. 380-385, ISSN 0304-3894

Zheng, W. Q., Zhang, J., Ge, Q. J., Xu, H. Y. & Li, W. Z. (2008). Effects of CeO_2 Addition on Ni/Al_2O_3 Catalysts for the Reaction of Ammonia Decomposition to Hydrogen. *Appl. Catal. B*, Vol.80, No.1-2, (April 2008), pp. 98-105, ISSN 0926-3373

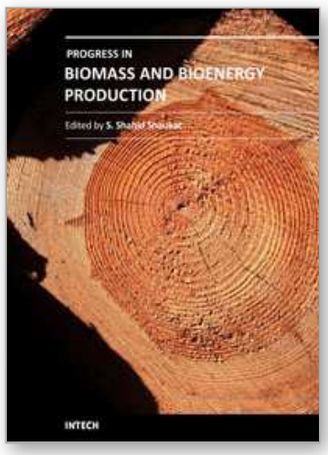

Progress in Biomass and Bioenergy Production
Edited by Dr. Shahid Shaukat

ISBN 978-953-307-491-7
Hard cover, 444 pages
Publisher InTech
Published online 27, July, 2011
Published in print edition July, 2011

Alternative energy sources have become a hot topic in recent years. The supply of fossil fuel, which provides about 95 percent of total energy demand today, will eventually run out in a few decades. By contrast, biomass and biofuel have the potential to become one of the major global primary energy source along with other alternate energy sources in the years to come. A wide variety of biomass conversion options with different performance characteristics exists. The goal of this book is to provide the readers with current state of art about biomass and bioenergy production and some other environmental technologies such as Wastewater treatment, Biosorption and Bio-economics. Organized around providing recent methodology, current state of modelling and techniques of parameter estimation in gasification process are presented at length. As such, this volume can be used by undergraduate and graduate students as a reference book and by the researchers and environmental engineers for reviewing the current state of knowledge on biomass and bioenergy production, biosorption and wastewater treatment.

INTECH
open science | open minds

InTech Europe
University Campus STeP Ri
Slavka Krautzeka 83/A
51000 Rijeka, Croatia
Phone: +385 (51) 770 447
Fax: +385 (51) 686 166
www.intechopen.com

InTech China
Unit 405, Office Block, Hotel Equatorial Shanghai
No.65, Yan An Road (West), Shanghai, 200040, China
中国上海市延安西路65号上海国际贵都大饭店办公楼405单元
Phone: +86-21-62489820
Fax: +86-21-62489821

IntechOpen